Draft version August 2, 2011
Preprint typeset using LaTeX style emulateapj v. 11/10/09

DISCOVERY OF A BRIGHT, EXTREMELY LOW-MASS WHITE DWARF IN A CLOSE DOUBLE DEGENERATE SYSTEM

S. Vennes[1,2], J. R. Thorstensen[3], A. Kawka[1], P. Németh[1,2], J. N. Skinner[3], A. Pigulski[4], M. Stęślicki[4], Z. Kołaczkowski[4], P. Śródka[4]

[1] Astronomický ústav, Akademie věd České republiky, Fričova 298, CZ-251 65 Ondřejov, Czech Republic
[3] Department of Physics and Astronomy, 6127 Wilder Laboratory, Dartmouth College, Hanover, NH 03755-352, USA and
[4] Instytut Astronomiczny, Uniwersytet Wrocławski, Kopernika 11, 51-622 Wrocław, Poland

Draft version August 2, 2011

ABSTRACT

We report the discovery of a bright ($V \sim 13.7$), extremely low-mass white dwarf in a close double degenerate system. We originally selected GALEX J171708.5+675712 for spectroscopic follow-up among a group of white dwarf candidates in an ultraviolet-optical reduced proper-motion diagram. The new white dwarf has a mass of $0.18\,M_\odot$ and is the primary component of a close double degenerate system ($P = 0.246137$ d, $K_1 = 288\,\mathrm{km\,s^{-1}}$) comprising a fainter white dwarf secondary with $M_2 \approx 0.9\,M_\odot$. Light curves phased with the orbital ephemeris show evidence of relativistic beaming and weaker ellipsoidal variations. The light curves also reveal secondary eclipses (depth ≈ 8 mmag) while the primary eclipses appear partially compensated by the secondary gravitational deflection and are below detection limits. Photospheric abundance measurements show a nearly solar composition of Si, Ca, and Fe ($0.1 - 1\,\odot$), while the normal kinematics suggest a relatively recent formation history. Close binary evolutionary scenarios suggest that extremely low mass white dwarfs form via a common-envelope phase and possible Roche-lobe overflow.

Subject headings: binaries: close — stars: individual (GALEX J171708.5+675712) — white dwarfs

1. INTRODUCTION

Many new members of the class of extremely low-mass (ELM) white dwarfs were discovered in the Sloan Digital Sky Survey (SDSS) and the Luyten surveys (e.g., Luyten Palomar, Luyten Half-Second, New Luyten Two-Tenths), such as SDSS J1234−0228 (Liebert et al. 2004), LP400-200 (Kawka et al. 2006), SDSS J0917+4638 (Kilic et al. 2007), and NLTT 11748 (Kawka & Vennes 2009). These objects are the products of close binary evolution and likely emerged from a common-envelope phase and possible Roche-lobe overflow (Nelemans et al. 2001). Some ELM white dwarfs are paired with a neutron star companion, e.g., the pulsar J1012+5307 (van Kerkwijk et al. 1996), implicating a range of initial secondary masses extending to $\gtrsim 8\,M_\odot$.

We have identified $\sim$ 200 bright hot subdwarf and white dwarf stars in a joint *Galaxy Evolution Explorer* (*GALEX*) ultraviolet (UV) survey and Guide Star Catalogue (GSC) survey (paper I: Vennes et al. 2011, and paper II: Nemeth et al., in preparation). A reduced proper-motion diagram based on the photographic color $V \sim V_{\rm GSC}$ ($H_V \equiv V + 5\log\mu + 5$) versus the color index $N_{\rm UV} - V_{\rm GSC}$ segregated the hot subdwarf and white dwarf candidates. As part of a second installment of our catalog of UV-selected stars, we identified GALEX J171708.5+675712 (hereafter, GALEX J1717+6757) as a likely white dwarf with $H_V \approx 12.3$.

We present photometric and spectroscopic observations (Section 2), and a model atmosphere and periodogram analysis showing GALEX J1717+6757 to be a new ELM white dwarf in a close binary and we analyze its photometric properties (Section 3). In Section 4, we estimate the distance, kinematics, and age of the system and discuss some implications for close binary evolutionary scenarios.

[2] Visiting Astronomer, Kitt Peak National Observatory, National Optical Astronomy Observatory, which is operated by the Association of Universities for Research in Astronomy (AURA) under cooperative agreement with the National Science Foundation.

2. OBSERVATIONS

We observed GALEX J1717+6757 on UT 2011 January 28 using the Ritchey-Chrétien Focus Spectrograph (RC-spec) attached to the 4-m telescope at Kitt Peak National Observatory (KPNO). We employed the T2KA CCD and the KPC-10A grating (316 lines per mm) with a dispersion of 2.75 Å per pixel in first order and centered on 5300 Å. We also inserted the order-sorting filter WG360 and covered a useful spectral range from 3600 to 7200 Å. The slit width was set at 1.5″ resulting in a spectral resolution of ≈ 5.5 Å. We obtained two consecutive exposures of 420 s each. A preliminary model atmosphere analysis revealed a relatively hot and subluminous object in a region of the HR diagram populated with ELM white dwarfs. We also measured a radial velocity $\sim 300\,\mathrm{km\,s^{-1}}$ indicating either peculiar kinematics or an orbital motion characterized by a large velocity amplitude.

We therefore obtained time series spectroscopy from 2011 March 18 to 21, using the 2.4-m Hiltner telescope and modular spectrograph (modspec) at MDM Observatory on Kitt Peak. A 1024^2 SITe CCD gave 2 Å pixel^{-1} and 3.5 Å resolution from 4660 to 6730 Å. We obtained a total of 65 exposures of 480 to 600 s each, spanning nearly 6 h of hour angle and covering all phases of the orbit, and measured radial velocities of the Hα and Hβ

TABLE 1
Photometry and astrometry.

Parameter	Measurement
GALEX $F_{\rm UV}$	13.44±0.10 mag
GALEX $N_{\rm UV}$	13.80±0.10 mag
SDSS u	13.548±0.003 mag
SDSS g	13.432±0.006 mag
SDSS r	13.441±0.003 mag
SDSS i	13.701±0.003 mag
SDSS z	13.987±0.004 mag
2MASS J	13.61±0.02 mag
2MASS H	13.69±0.03 mag
2MASS K	13.64±0.05 mag
R.A. (J2000)	17 17 08.865
Dec. (J2000)	+67 57 11.33
$\mu_\alpha \cos\delta$	-6.7 ± 2.2 mas yr^{-1}
μ_δ	51.6 ± 0.5 mas yr^{-1}

lines using a convolution algorithm (Schneider & Young 1980). We also obtained eight velocities using the same setup 2011 June 21 through 25 to further constrain the ephemeris (Section 3.2).

Next, we obtained Johnson BVI photometric time series on 2011 February 8 and 21, and March 19 and 22, using the 0.6-m telescope at Białków Observatory. The exposure times were 60 s in V and I, and 100 s in B. The data were corrected for second-order extinction effects by fitting a line to the differential magnitude versus air-mass diagram and subsequently removing the linear dependence. Each time series provided approximately 5 hours of continuous coverage in the three photometric bands. We also obtained high signal-to-noise ratio white-light time series on 2011 June 2, 3, 4, 6, and 7 with exposure times of 30 s. The time series provided between 2 to 5 hours of continuous coverage.

Finally, we collected photometric measurements from the SDSS (Abazajian et al. 2009), 2 Micron All-Sky Survey (2MASS, Skrutskie et al. 2006) and *GALEX* survey (Table 1). We corrected the *GALEX* photometry for non-linearity (Morrissey et al. 2007) and estimated an error of 0.1 mag in the process. These measurements are useful in building a spectral energy distribution (SED) and in constraining the atmospheric parameters of the white dwarf (Section 3.1). The SDSS g-band photometric measurement shows discrepancy with other photometric measurements and was rejected from the SED. Table 1 lists astrometric measurements from the Third U.S. Naval Observatory CCD Astrograph Catalog (Zacharias et al. 2010) that will be used to determine the kinematical properties of GALEX J1717+6757 (Section 4).

3. ANALYSIS

3.1. *Properties of the primary*

We computed a grid of models in non-local thermodynamic equilibrium (non-LTE) using Tlusty-Synspec (Hubeny & Lanz 1995; Lanz & Hubeny 1995) versions 200 and 48, respectively. When fitting the Balmer lines (Hα to H13), the best-fitting parameters

$$T_{\rm eff} = 14\,900 \pm 200 \text{ K}, \quad \log g = 5.67 \pm 0.05,$$

and a low helium abundance $\log{[n({\rm He})/n({\rm H})]} < -2.3$ ($< 0.05\,\odot$, where $\odot$ is the solar abundance relative to hydrogen) confirmed the nature of GALEX J1717+6757 as an ELM white dwarf. Using these parameters we estimated the absolute magnitude in the Sloan r band $M_r = 6.99 \pm 0.08$, and with the corresponding distance modulus $r - M_r = 6.45 \pm 0.08$ ($r = 13.441$) we estimated a distance of 195 ± 7 pc. Figure 1 shows the SED and best-fitting non-LTE model; GALEX J1717+6757 lies toward a low-density line-of-sight in the interstellar medium ($E_{B-V} \approx 0.03$ mag, Schlegel et al. 1998) with negligible extinction in the intervening medium. The mass and age of the white dwarf may be estimated by locating it on the evolutionary tracks with solar metallicity (Serenelli et al. 2001) or with low metallicity ($Z = 0.001$, Serenelli et al. 2002). The mass is model-dependent and the error is dominated by the choice of the model grid. Using low-metallicity models we find $M_1 = 0.184 \pm 0.001 M_\odot$, but the mass derived from solar-metallicity models is less certain because of a large gap between the 0.169 and $0.196 M_\odot$ sequences. Extrapolating from the sequence of low mass models ($0.148, 0.160, 0.169 M_\odot$) the mass is estimated at $0.185 M_\odot$. Based on these two model sequences and considering that the ELM lies within the available sequences, i.e., 0.169 and $0.196 M_\odot$, we conservatively estimate $M_1 = 0.185 \pm 0.010 M_\odot$ and $R_1 = 0.10 \pm 0.01 R_\odot$ for both low- and high-metallicity models. We examine the age problem in Section 4.

The surface composition of GALEX J1717+6757 is that of a heavily polluted white dwarf. Figure 1 (inset) shows photospheric heavy element lines that are suitable for abundance measurements. Formally classified as DAZ white dwarfs, the hydrogen-rich white dwarfs with heavy-element spectral lines constitute approximately 20% of the DA population (Zuckerman et al. 2003; Koester et al. 2005). We fitted the Ca IIλ3933, Fe II$\lambda\lambda$4923, 5018, 5169, and Si II$\lambda\lambda$5041,5056,6347,6371 Å lines with high-metallicity non-LTE models computed using Tlusty-Synspec and measured:

$$\log{[n({\rm Si})/n({\rm H})]} = -5.5 \pm 0.3 \ (0.1\,\odot),$$
$$\log{[n({\rm Ca})/n({\rm H})]} = -5.7 \pm 0.3 \ (1.0\,\odot),$$
$$\log{[n({\rm Fe})/n({\rm H})]} = -5.1 \pm 0.3 \ (0.3\,\odot).$$

The atmospheric composition is somewhat below the solar composition, with a helium abundance less than 5% of the solar abundance. High-dispersion and high signal-to-noise ratio spectra are required to constrain the abundance of other heavy elements. The origin of these heavy elements may be fossil or accreted from the immediate circumstellar environment (see a discussion by Koester & Wilken 2006). A direct link to the metallicity of the progenitor cannot be established because the surface composition of white dwarf stars is determined by diffusion processes characterized by time-scales much shorter than evolutionary time-scales.

3.2. *Binary properties and nature of the secondary*

A periodogram constructed from the radial velocities, selected an unambiguous period, and a sinusoidal fit of the form $v(t) = \gamma + K \sin[2\pi(t - T_0)/P]$ gave

$$T_0 = \text{HJD } 2455641.9309 \pm 0.0004,$$

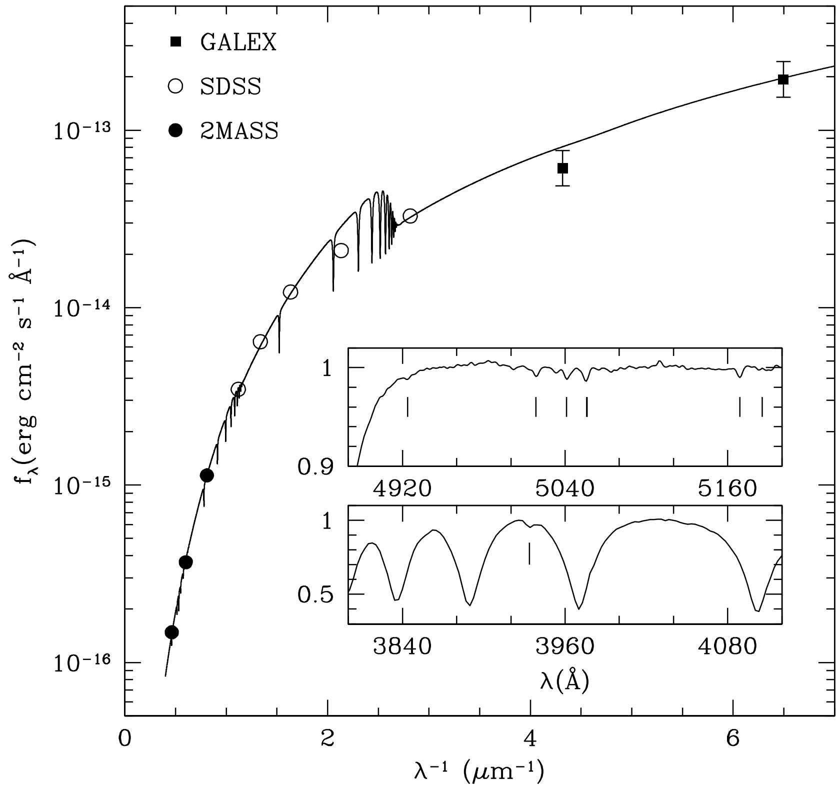

FIG. 1.— Spectral energy distribution (2MASS JHK, SDSS *ugriz*, *GALEX* N_{UV} and F_{UV}) of GALEX J1717+6757 compared to the best-fitting model 14 900 K and $\log g = 5.67$. The effect of minimal extinction ($E_{B-V} = 0.005$ mag) is added to the model. In the inset, the co-added KPNO spectrum shows the upper Balmer lines and a weak photospheric Ca IIλ3933 line, and the co-added MDM spectrum shows Si IIλλ5041, 5056, 5186 and Fe IIλλ4923, 5018, 5169 lines.

$$P = 0.246137 \pm 0.000003 \text{ d},$$
$$K = 288 \pm 2 \text{ km s}^{-1},$$
$$\gamma = -21.3 \pm 1.7 \text{ km s}^{-1},$$

with an RMS residual of only 8 km s^{-1}. The initial epoch T_0 corresponds to the inferior conjunction of the primary.

Figure 2 shows the spectroscopic trail obtained at MDM Observatory: Hα and Si IIλλ6347, 6371 clearly trace the primary orbit bolstering the photospheric identification of the silicon lines. We found no spectroscopic signatures of the faint secondary star. The folded radial velocity curve follows a circular orbit (Fig. 2).

The period and K-velocity imply a mass function for the secondary

$$f(M_2) = 0.609 \pm 0.012\, M_\odot,$$

or, assuming $M_1 = 0.185 \pm 0.010\, M_\odot$, $M_2 \gtrsim 0.86\, M_\odot$, so the companion must be a compact object. If the unseen companion is below the Chandrasekhar limit $M_2 \lesssim 1.35\, M_\odot$, then the inclination $i \gtrsim 60°$. No radio sources are found in the vicinity of the ELM white dwarf in the NRAO-VLA Sky Survey (NVSS) with a sensitivity of ~ 0.5 mJy at 1400 MHz (Condon et al. 1998), contrasting with the detection of the milli-second pulsar PSR J1012+5307 in the NVSS (Kaplan et al. 1998) and other radio observations (Nicastro et al. 1995). Pulsar companions to ELM white dwarfs are relatively rare (Agüeros et al. 2009) and we conclude that the companion to the ELM white dwarf GALEX J1717+6757 is a massive white dwarf.

We folded the Białków photometric time series on our ephemeris. Including all V data, the time series folded on half the period has a weak amplitude of 1.5 ± 0.4 mmag and a maximum at phase 0.30 ± 0.02 (statistical error only), i.e. close to phase 0.25 expected for ellipticity effect. Using "JKTEBOP"[5] (Popper & Etzel 1981) we verified that the amplitude calculated from the model for the system parameters agrees with the observed amplitude. The V time series folded on the period has a stronger amplitude of 2.2 ± 0.4 mmag with a maximum at phase 0.81 ± 0.03, i.e., also $\approx 2\sigma$ from phase 0.75 expected for relativistic beaming. Figure 3 shows the folded V time-series and a model curve combining both effects: we added stellar distortion with an amplitude of 1.5 mmag and relativistic beaming with an amplitude of 2.2 mmag. van Kerkwijk et al. (2010) and Shporer et al. (2010) discuss the beaming effect in close binaries; because the primary outshines the secondary, the amplitude of the effect can be written simply as $A \approx \alpha\, e^\alpha/(e^\alpha - 1) \times (K/c)$, where c is the speed of light, K ($= 288\,\text{km}\,\text{s}^{-1}$) the velocity semi-amplitude, and $\alpha = h\nu/kT_{\text{eff}}$ where ν is the frequency of the photometric bandpass and T_{eff} is the stellar effective temperature. In the V band, the amplitude of the effect in GALEX J1717+6757 is expected to be $A = 2.3$ mmag. This is the second star in which

[5] Available at `http://www.astro.keele.ac.uk/~jkt/codes/jktebop.html`

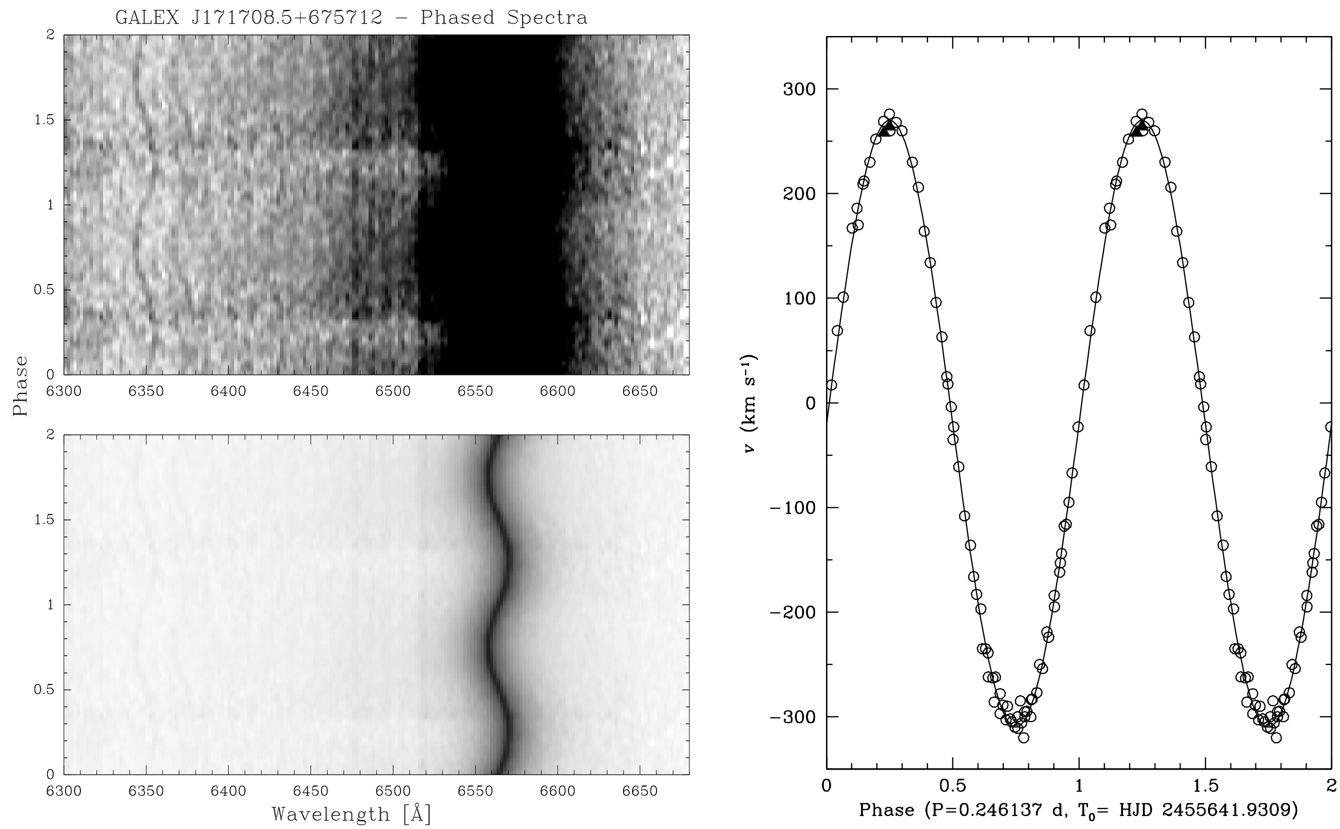

Fig. 2.— (Left) trailed spectra showing Si II$\lambda\lambda$6347, 6371 and Hα lines tracing the orbital motion (Section 3.2) of the bright ELM white dwarf primary. The upper panel is scaled to bring out the Si II features, and the lower to show the core of the Hα line. (Right) radial velocity measurements phased on the orbital period with the best-fitting sinusoidal curve tracing the primary orbital motion. The data are repeated for one cycle for continuity. The full triangles near phase 0.2 are from the Kitt Peak 4 m, and all other velocities are from the MDM 2.4 m.

relativistic beaming was detected from the ground after NLTT 11748 (Shporer et al. 2010).

Adopting for the primary and secondary $M_1 = 0.185M_\odot$, $R_1 = 0.1R_\odot$ (Section 3.1) and $M_2 = 0.9M_\odot$, $R_2 = 0.008R_\odot$ (using mass-radius relations of Benvenuto & Althaus 1999), respectively, the secondary eclipse would last up to 400 s at $i = 90°$ with a depth of 7 mmag assuming an identical surface flux for the primary and secondary stars. Employing only the June data (white light) we observed four secondary eclipses at T(HJD 2455000+) = 715.5252, 716.5098, 717.4944, and 720.4476, and lasting on average 80-150 s ($i = 86.75 \pm 0.05°$) with a depth of 8 mmag. The eclipse times are consistent with phase = 0 with an offset of only -0.003 ± 0.004, and suggest only a small adjustment to the orbital period of -0.0000025 d, i.e., within quoted errors. Figure 3 shows the white-light time series phased with the adjusted period. The primary eclipse, i.e., the transit of the secondary, is not clearly detected with a maximum depth of ≈ 4 mmag. The primary eclipse is partially compensated by gravitational deflection by the massive white dwarf. With the adopted parameters and a binary separation of $1.7R_\odot$, the Einstein radius of the secondary is $R_E = 0.0036R_\odot$. The total transit depth including the lensing effect may be written as (Marsh 2001) $\Delta m \approx (R_2/R_1)^2 - 2(R_E/R_1)^2$, where "1" designates the ELM primary, and "2" the massive unseen companion. Consequently, the predicted transit is $\Delta m \approx 4$ mmag, consistent with the deepest feature found at phase 0.5. This lensing effect has been observed in NLTT 11748 (Steinfadt et al. 2010).

4. DISCUSSION

The ELM GALEX J1717+6757 constitutes an interesting test of evolutionary models. Following low-metallicity evolutionary tracks, the white dwarf has a cooling age of 880^{+40}_{-30} Myr, but it is not possible to derive an age using the solar-metallicity tracks due to a large gap in properties above $0.169M_\odot$. Figure 4 compares the evolutionary models to samples of ELM white dwarfs. We selected the old systems LP 400-22 (Kawka et al. 2006; Kilic et al. 2009; Vennes et al. 2009), NLTT 11748 (Kawka & Vennes 2009; Steinfadt et al. 2010; Kawka et al. 2010) and a sample of low-mass white dwarfs in the SDSS survey (Kulkarni & van Kerkwijk 2010; Brown et al. 2010; Kilic et al. 2011a,b). The ELM precursor HD 188112 (Heber et al. 2003) is also shown with a pre-flash model describing low-mass subdwarf stars (Driebe et al. 1998). The evolutionary tracks cover the population with masses ranging from $\gtrsim 0.15M_\odot$ to $\approx 0.45M_\odot$. The ELM white dwarfs ($M \lesssim 0.2M_\odot$) occupy a relatively high-luminosity region of the diagram characterized by residual burning. Althaus et al. (2001) estimates that, taking into account the effect of diffusion, objects with masses $\gtrsim 0.18M_\odot$ will experience a thermonuclear flash that delays their cooling. The effect is also metallicity dependent, with higher-metallicity objects experiencing a flash at a comparatively lower

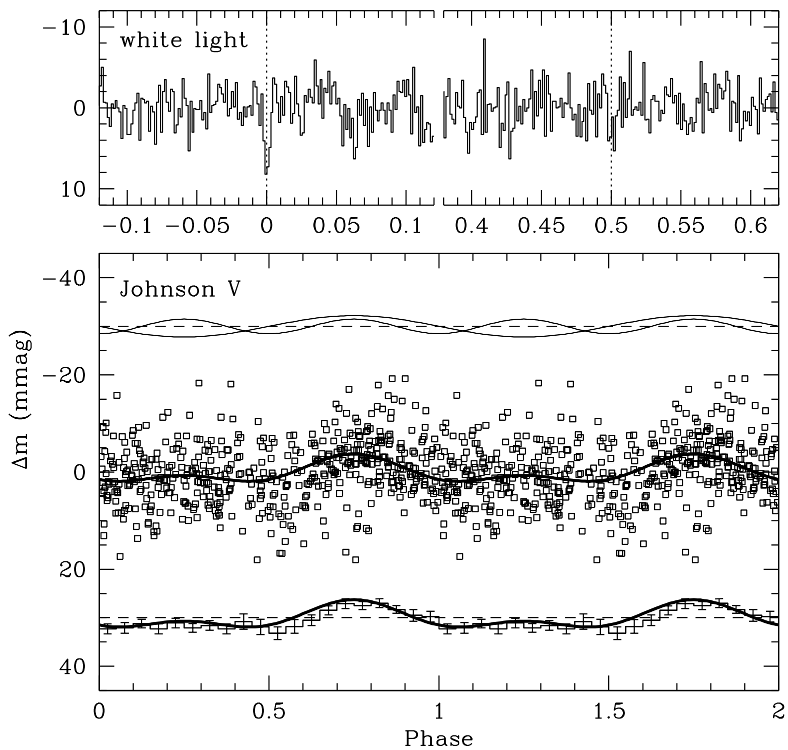

Fig. 3.— (Top panel) white-light time series (30 s bins) folded on the ephemeris (see text) covering the primary (phase = 0.5) and secondary (phase = 0) eclipses, and (bottom panel) Johnson V time series (open squares) and model curve (thick line). The upper curves in the bottom panel are offset by −30 mmag and depict ellipsoidal effect at half-period and relativistic beaming at full-period (see text), while the lower curves are offset by 30 mmag and represent the binned (0.05 phase) light-curve (histogram with error bars) and the model curve (thick line).

mass. Independent age and mass estimates are possible in binaries comprising an ELM white dwarf and a pulsar (see Althaus et al. 2001) but are more difficult to obtain in double white dwarf systems. The ELM GALEX J1717+6757 is one of the youngest known class members, but the estimated age of the system remains model-dependent with the metallicity of the progenitors still unconstrained.

The ELM primary in GALEX J1717+6757, with an estimated radius $R_1 = 0.1\,R_\odot$ fills in only about 1.2% of its Roche volume ($R_{1,L} = 0.43\,R_\odot$, following Eggleton 1983) resulting in low-amplitude ellipsoidal variations compounded with a dominant relativistic beaming effect. The system is expected to merge ($t_{\rm merge}$) in 7.0 Gyr assuming a secondary mass $M_2 = 0.9\,M_\odot$ (Ritter 1986), and the product of the merger will likely be an ultramassive white dwarf with $M \approx 1.1\,M_\odot$.

Using a distance $d = 195 \pm 7$ pc (Section 3.1), and the velocity and proper motion measurements we computed the (U,V,W) velocity vector following Johnson & Soderblom (1987):

$$(U,V,W) = (-35\pm3, -21\pm3, -8\pm3)\ {\rm km\,s^{-1}}.$$

The velocity components are characteristic of the thin Galactic disc and similar to the white dwarf population in general (Sion et al. 1988; Pauli et al. 2006). We conclude that unlike the old systems LP 400-22 and NLTT 11748 that show peculiar kinematics, the system GALEX J1717+6757 is kinematically young. The calculation of additional evolutionary tracks covering the observed range of parameters, particularly between 0.17 and 0.19 $M_\odot$, would benefit studies of ELM white dwarfs and their likely progenitors.

S.V. and A.K. are supported by GA AV grant numbers IAA300030908 and IAA301630901, respectively, and by GA ČR grant number P209/10/0967. A.K. also acknowledges support from the Centre for Theoretical Astrophysics (LC06014). J.R.T. and J.N.S acknowledge support from NSF grant AST-0708810. A.P. and Z.K. acknowledge Polish MNiSzW grant N N203 302635. This research has made use of the VizieR catalogue access tool (CDS, Strasbourg, France), and of data products from the Two Micron All Sky Survey which is a joint project of the University of Massachusetts and the Infrared Processing and Analysis Center/California Institute of Technology, funded by the National Aeronautics and Space Administration and the National Science Foundation.

Facilities: GALEX, Mayall.

REFERENCES

Abazajian, K. N., et al. 2009, ApJS, 182, 543

Agüeros, M. A., et al. 2009, ApJ, 700, L123

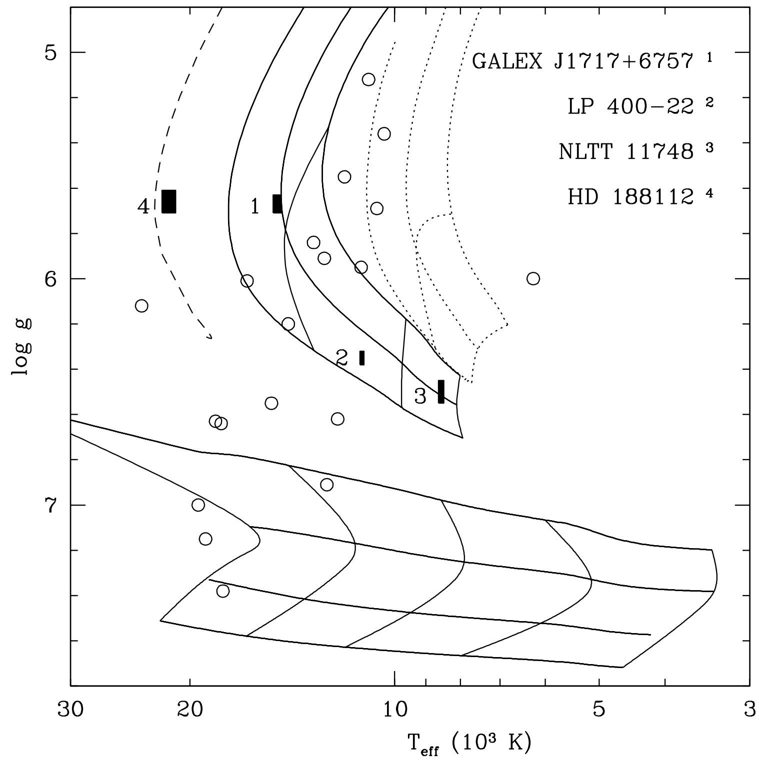

Fig. 4.— Sample of low-mass white dwarfs (open circles, see text) and selected ELM white dwarfs (full rectangles covering error bars) and evolutionary tracks in the ($T_{\rm eff}$, $\log g$) plane. The dashed line shows a pre-flash model at $0.234M_\odot$ (Driebe et al. 1998). The full lines show a series of low-metallicity models at, from top to bottom, 0.172, 0.183 and $0.197M_\odot$ drawn with isochrones at, from right to left, 10, 3, and 1 Gyr, and, from the same grid, models at 0.244, 0.300, 0.380, and $0.449M_\odot$ with isochrones, from right to left, at 10, 3, 1, 0.3, and 0.1 Gyr (Serenelli et al. 2002). The dotted lines show solar-metallicity models at, from top to bottom, 0.148, 0.160, and $0.169M_\odot$ with isochrones, from right to left, at 10 and 3 Gyr (Serenelli et al. 2001).

Althaus, L. G., Serenelli, A. M., & Benvenuto, O. G. 2001, MNRAS, 324, 617
Benvenuto, O. G., & Althaus, L. G. 1999, MNRAS, 303, 30
Brown, W. R., Kilic, M., Allende Prieto, C., & Kenyon, S. J. 2010, ApJ, 723, 1072
Condon, J. J., Cotton, W. D., Greisen, E. W., Yin, Q. F., Perley, R. A., Taylor, G. B., & Broderick, J. J. 1998, AJ, 115, 1693
Driebe, T., Schoenberner, D., Bloecker, T., & Herwig, F. 1998, A&A, 339, 123
Eggleton, P.P. 1983, ApJ, 268, 368
Heber, U., Edelmann, H., Lisker, T., & Napiwotzki, R. 2003, A&A, 411, L477
Hubeny I., Lanz T., 1995, ApJ, 439, 875
Johnson, D. R. H., & Soderblom, D. R. 1987, AJ, 93, 864
Kaplan, D. L., Condon, J. J., Arzoumanian, Z., & Cordes, J. M. 1998, ApJS, 119, 75
Kawka, A., & Vennes, S. 2009, A&A, 506, L25
Kawka, A., Vennes, S., Oswalt, T. D., Smith, J. A., & Silvestri, N. M. 2006, ApJ, 643, L123
Kawka, A., Vennes, S., & Vaccaro, T. R. 2010, A&A, 516, L7
Kilic, M., Allende Prieto, C., Brown, W. R., & Koester, D. 2007, ApJ, 660, 1451
Kilic, M., et al. 2011a, MNRAS, 413, L101
Kilic, M., Brown, W. R., Allende Prieto, C., Agüeros, M. A., Heinke, C., & Kenyon, S. J. 2011b, ApJ, 727, 3
Kilic, M., Brown, W. R., Allende Prieto, C., Swift, B., Kenyon, S. J., Liebert, J., & Agüeros, M. A. 2009, ApJ, 695, L92
Koester, D., Rollenhagen, K., Napiwotzki, R., Voss, B., Christlieb, N., Homeier, D., & Reimers, D. 2005, A&A, 432, 1025
Koester, D., & Wilken, D. 2006, A&A, 453, 1051
Kulkarni, S. R., & van Kerkwijk, M. H. 2010, ApJ, 719, 1123
Lanz T., Hubeny I., 1995, ApJ, 439, 905
Liebert, J., Bergeron, P., Eisenstein, D., Harris, H. C., Kleinman, S. J., Nitta, A., & Krzesinski, J. 2004, ApJ, 606, L147
Morrissey P., et al., 2007, ApJS, 173, 682
Marsh, T. R. 2001, MNRAS, 324, 547
Nelemans, G., Yungelson, L. R., Portegies Zwart, S. F., & Verbunt, F. 2001, A&A, 365, 491
Nicastro, L., Lyne, A. G., Lorimer, D. R., Harrison, P. A., Bailes, M., & Skidmore, B. D. 1995, MNRAS, 273, L68
Pauli, E.-M., Napiwotzki, R., Heber, U., Altmann, M., & Odenkirchen, M. 2006, A&A, 447, 173
Popper, D. M., & Etzel, P. B. 1981, AJ, 86, 102
Ritter, H. 1986, A&A, 169, 139
Schlegel, D. J., Finkbeiner, D. P., & Davis, M. 1998, ApJ, 500, 525
Schneider, D. P., & Young, P. 1980, ApJ, 238, 946
Serenelli, A. M., Althaus, L. G., Rohrmann, R. D., & Benvenuto, O. G. 2001, MNRAS, 325, 607
Serenelli, A. M., Althaus, L. G., Rohrmann, R. D., & Benvenuto, O. G. 2002, MNRAS, 337, 1091
Shporer, A., Kaplan, D. L., Steinfadt, J. D. R., Bildsten, L., Howell, S. B., & Mazeh, T. 2010, ApJ, 725, L200
Sion, E. M., Fritz, M. L., McMullin, J. P., & Lallo, M. D. 1988, AJ, 96, 251
Skrutskie, M. F., et al. 2006, AJ, 131, 1163
Steinfadt, J. D. R., Kaplan, D. L., Shporer, A., Bildsten, L., & Howell, S. B. 2010, ApJ, 716, L146
van Kerkwijk, M. H., Bergeron, P., & Kulkarni, S. R. 1996, ApJ, 467, L89
van Kerkwijk, M. H., Rappaport, S. A., Breton, R. P., Justham, S., Podsiadlowski, P., & Han, Z. 2010, ApJ, 715, 51
Vennes, S., Kawka, A., Vaccaro, T. R., & Silvestri, N. M. 2009, A&A, 507, 1613
Vennes, S., Kawka, A., & Németh, P. 2011, MNRAS, 410, 2095
Zacharias, N., et al. 2010, AJ, 139, 2184
Zuckerman, B., Koester, D., Reid, I. N., Hünsch, M. 2003, ApJ, 596, 477